Modeling bubbles and droplets in magnetic fluids

2008 J. Phys.: Condens. Matter 20 204143

(http://iopscience.iop.org/0953-8984/20/20/204143)

IOP PUBLISHING JOURNAL OF PHYSICS: CONDENSED MATTER

J. Phys.: Condens. Matter **20** (2008) 204143 (5pp) doi:10.1088/0953-8984/20/20/204143

Modeling bubbles and droplets in magnetic fluids

Mark S Korlie, Arup Mukherjee, Bogdan G Nita, John G Stevens, A David Trubatch and Philip Yecko

Department of Mathematical Sciences, Montclair State University, 1 Normal Avenue, Montclair, NJ 07043, USA

E-mail: philip.yecko@montclair.edu

Received 30 June 2007
Published 1 May 2008
Online at stacks.iop.org/JPhysCM/20/204143

Abstract

We develop, test and apply a volume of fluid (VOF) type code for the direct numerical simulation of two-fluid configurations of magnetic fluids with dynamic interfaces. Equilibrium magnetization and linear magnetic material are assumed and uniform imposed magnetic fields are considered, although extensions to nonlinear materials and to fields with spatio-temporal variability are possible. Models are computed for configurations of bubbles of non-magnetic fluid rising in ferrofluid and droplets of ferrofluid falling through non-magnetic fluid. Bubbles and droplets exhibit similar changes of shape in the presence of vertical fields, due to a combination of elongation along the field lines and the fluid dynamics of ordinary rising or falling at small Bond number. Bubbles become more prolate than droplets under the same parameters and are accordingly found to break up more readily than droplets in stronger fields. Indirect effects are observed, such as the change in rise time and the consequent changes in the flow due to increased Reynolds number.

(Some figures in this article are in colour only in the electronic version)

1. Introduction

Many configurations of magnetic fluids include an interface separating the fluid from a second medium, such as air or another liquid. As in the non-magnetic case, there is both practical and academic interest in those interfacial flows involving layers, sheets, jets, droplets and bubbles. Aside from the jump in density and viscosity generally found at fluid interfaces, in a magnetic fluid (ferrofluid) there will usually be a jump in magnetic properties. A notable case in point is the normal field instability [5] that has become a hallmark of the discipline of ferrohydrodynamics. Bubbles and droplets are ubiquitous in industrial and natural flows and often have a significant impact on the physical properties of the flow.

In this work we focus on configurations involving either a single bubble of non-magnetic material in a ferrofluid or a single droplet of ferrofluid immersed in a non-magnetic fluid. A bubble with lower density than its surroundings will rise under gravity with possibly complicated trajectory and change of shape as dictated by the viscosity ratio, Bond number and Morton number (defined below). A droplet of higher density will fall through its surroundings, but along a straight trajectory. In both cases, an imposed magnetic field, even if steady and uniform, can modify both shape and trajectory. If the densities of the fluids are matched (or if gravity is absent) a uniform magnetic field leads to an equilibrium shape in which the droplet or bubble elongates along the field lines. In this work, our interest is in dynamic behavior as opposed to static equilibria. For another extreme, we examine the conditions under which breakup of a bubble or droplet will occur.

The study of the equilibrium shape of a neutrally buoyant ferrofluid droplet in a uniform field has a long history [19, 18, 1] and includes the mathematical analog of a dielectric droplet in a uniform electric field [19, 18, 14, 20, 6, 8]. It was realized early [6, 8] that the influence of the magnetic field stemmed from the Maxwell stress and could be reduced to a normal stress acting at the interface. This stress depends on the normal and tangential components of the magnetic field at the interface and can be shown to be largest at the two poles (where the axis is the field direction) of the bubble or droplet. To maintain a normal stress balance, the curvature increases at the poles and decreases at the equator, leading to a prolate shape. That a prolate shape results no matter which fluid has the higher permeability was

first explained in [6, 8] for dielectric fluids and explained and experimentally validated for ferrofluids by [1].

In this work we use direct numerical simulations to study static and dynamic ferrofluid bubbles and droplets. The numerical modeling of incompressible fluids with interfaces is a broad problem with many approaches (see [17] for a review). One of the more successful and robust approaches, interface capturing, treats the multi-component fluid as a single fluid with abrupt changes in density and viscosity, using an auxiliary function to capture the interface. The two most common interface capturing methods are the *level set* method, in which the interface is the zero contour of a smooth function, and the *volume of fluid* or *VOF* method, in which a color (or phase) function describes which fluid occupies each computational cell. Level set methods naturally allow precise computation of the interface's geometric properties, such as its normal and curvature, yet tend to conserve volume (mass) poorly. VOF methods, on the other hand, naturally conserve volume accurately, but lead to inaccurate curvature estimates. The inaccurate curvatures of VOF methods are one source of so-called spurious current errors [17]. For this work we have developed a VOF method as an extension of the SURFER code [7] in which magnetic interfacial stresses and solution of the magnetostatic Maxwell equations have been incorporated. Other workers have approached ferrofluid interface modeling using different methods [11].

2. Governing equations

Here we consider only configurations involving one non-magnetic fluid and one magnetic fluid, of permeability μ and susceptibility $\chi = \mu/\mu_0 - 1$. We further assume a linear magnetic material (μ, χ constant) and equilibrium magnetization, $\mathbf{M} = \mathbf{M}_0 = \chi\mathbf{H}$ such that $\mathbf{M} \times \mathbf{H} = 0$. Maintaining consistency with the VOF approach, we treat this multi-component fluid as a single fluid with spatially varying density, viscosity and magnetic permeability.

Neglecting striction this leads to a modified Navier–Stokes governing equation

$$\rho\left(\frac{\partial \mathbf{u}}{\partial t} + \mathbf{u}\cdot\nabla\mathbf{u}\right) = -\nabla p + \rho\mathbf{g} + \eta\nabla^2\mathbf{u} - \frac{1}{2}\mathbf{H}\cdot\mathbf{H}\nabla\mu, \quad (1)$$

where $\mathbf{g}$ is gravity and we assume isothermal and incompressible media,

$$\nabla\cdot\mathbf{u} = 0. \quad (2)$$

In the form (1) the pressure, p, represents the hydrodynamic pressure only. The magnetic forces are captured in the rightmost term, which will vanish in the bulk of the fluid where μ is constant, but act on the interface where μ jumps in value [15, 12].

The (magnetostatic) Maxwell's equations, $\nabla\times\mathbf{H} = 0$ and $\nabla\cdot\mathbf{B} = 0$, where $\mathbf{B} = \mu_0(\mathbf{H}+\mathbf{M})$, are more conveniently posed in terms of a magnetic potential ϕ,

$$\nabla\cdot([1+\chi]\nabla\phi) = 0 \quad (3)$$

where $\mathbf{H} = \nabla\phi$. Equation (3) is also solved in a single domain in which χ varies sharply at the interface. In this way, the conditions that normal $\mathbf{B}$ and tangential $\mathbf{H}$ remain continuous are naturally captured by the solution.

The coupling of the magnetic field reduces to a singular normal force acting on the interface, just as for the force of interfacial tension. We are then able to describe a two-fluid system with a dynamic interface using the single equation

$$\rho\left(\frac{\partial \mathbf{u}}{\partial t} + \mathbf{u}\cdot\nabla\mathbf{u}\right) = -\nabla p + \rho\mathbf{g} + \eta\nabla^2\mathbf{u} + \sigma\kappa\,\delta_S\mathbf{n} + \mathcal{F}_\mathrm{M}\delta_S \quad (4)$$

where δ_S is a distribution identifying the interface and $\mathbf{n}$ is the interface normal; also, σ is the interfacial tension coefficient, κ is the interface curvature and $\mathcal{F}_\mathrm{M}$ is the magnetic interfacial force. Magnetic interfacial force is defined in terms of the jump in magnetic normal stress at the interface

$$\mathcal{F}_\mathrm{M} = \left[\mathbf{n}\cdot\left(\mu\mathbf{H}\mathbf{H} - \frac{\mu}{2}H^2\mathbb{I}\right)\right] \quad (5)$$

where the square brackets represent the difference taken across the interface. The solution of equation (3) can be used to evaluate the field in the neighborhood of the interface. Alternatively, one can use the continuity of normal $\mathbf{B}$ and tangential $\mathbf{H}$ to find more convenient expressions for the magnetic interfacial force.

The equilibrium magnetic field internal to an ellipsoidally shaped interface is uniform and has a well known exact solution [9]. It can be shown [14] that any axisymmetrically shaped bubble or droplet has a uniform internal field.

Rosensweig has found an expression in terms of the magnetization, namely $\mathcal{F}_\mathrm{M} = -\frac{\mu_0}{2}(\chi\mathbf{H}\cdot\mathbf{H} + \chi^2 H_\mathrm{n}^2)$ where H_n is the component of magnetic field normal to the interface [15]. The above expression is convenient but does not easily reveal the competing effect of the normal and tangential field components. Garton and Krasucki [6] have derived an expression for the interfacial force acting in perfect dielectric fluids [6]. Following that work, we can find an analogous expression for magnetic fluids, $\mathcal{F}_\mathrm{M} = \frac{1}{2}(\mu_\mathrm{i}-\mu_\mathrm{o})[H_\mathrm{t}^2 + \frac{\mu_\mathrm{i}}{\mu_\mathrm{o}}H_\mathrm{n}^2]_\mathrm{i}$, where the subscripts i and o refer to *inner* and *outer* and t indicates the *tangential* component. This expression clearly shows that the difference $\mu_\mathrm{i} - \mu_\mathrm{o}$ determines the sign of the magnetic interfacial force, while the ratio $\mu_\mathrm{i}/\mu_\mathrm{o}$ determines the relative importance of the normal field component. Notice that even though the above interfacial force is of opposite sign in bubbles and droplets, it increases poleward in both cases, making time independent solutions for both bubbles and droplets have a prolate shape. In the next section we describe the numerical technique used to solve equations (2), (4) and (3) numerically.

3. Computational method

The above equations are solved numerically by extending the SURFER code to include the magnetic interfacial force (the rightmost term of equation (4)), and a multigrid relaxation algorithm to solve (3). Details of each of these extensions follow.

3.1. Interface normal

In SURFER the interface is captured using a color function C with values in [0, 1] which is used to track the identity of fluid inside each computational box (node). Note that C is simply advected, namely: it satisfies

$$\frac{\partial C}{\partial t} + \mathbf{u} \cdot \nabla C = 0, \tag{6}$$

and that $C_{ij} = 0$ in fluid 1, $C_{ij} = 1$ in fluid 2 and $0 < C_{ij} < 1$ represents the fraction of a grid box that is occupied by fluid 2, which is found only in boxes through which the interface cuts.

A discrete interface normal can be computed using $\mathbf{n} = \nabla C/|\nabla C|$; a version of the Parker–Youngs normal [16] defines the components of $\mathbf{n}$ as follows:

$$n^x_{i,j} = \frac{1}{h}(C_{i+1,j+1} + 2C_{i+1,j} + C_{i+1,j-1} - C_{i-1,j+1} - 2C_{i-1,j} - C_{i-1,j-1}),$$

$$n^y_{i,j} = \frac{1}{h}(C_{i+1,j+1} + 2C_{i,j+1} + C_{i-1,j+1} - C_{i+1,j-1} - 2C_{i,j-1} - C_{i-1,j-1}) .$$

Since the computation of curvature is not required for magnetic forces, curvature algorithms are not discussed here but can be found in [17]. Other methods have also been used [10].

3.2. Magnetostatic Maxwell equation

In terms of the color function C, the material properties in the single-fluid approach are defined as follows: $\rho = \rho_1 C + (1 - C)\rho_2$, $\eta = \eta_1 C + (1 - C)\eta_2$ and $\chi = \chi_1 C + (1 - C)\chi_2$.

The solution of the equation (3) is made difficult by the fact that the coefficient, $1 + \chi$, experiences a jump at the interface. To alleviate this we apply a standard V-cycle multigrid algorithm on several levels of increasingly coarse grids, using the previous time solution for ϕ as an initial guess on the finest grid. At each level we use a simple red–black Gauss–Seidel iteration; on the coarsest grid, up to fifty iterations are required but the size of the problem is small. The multigrid method converges once the residual (error) becomes smaller than a fixed tolerance; otherwise an additional V-cycle is performed.

4. Direct numerical simulations

Here we show first a numerical resolution study at low field strength followed by results for the cases of a bubble of non-magnetic fluid rising buoyantly through a ferrofluid and a falling droplet of ferrofluid. For both bubbles and droplets a uniform vertical magnetic field is imposed and the simulations are two-dimensional. Extension to three-dimensional simulations is straightforward but requires a requisite increase in computing resources. Rising bubbles (and falling droplets) can be characterized in terms of their Bond (or Eötvös) and Morton numbers [4]. The Morton number, Mo is a material quantity (for water at room temperature, $Mo = 3 \times 10^{-11}$) and is very small in our simulations. The Bond number is defined as $Bo := g\Delta\rho d^2/\sigma$, where d is the bubble size; Bo measures the relative importance of buoyancy and interfacial tension. Bubbles having $Bo < 1$ remain approximately spherical as they rise. In our simulations we keep the Bond number near unity. Because of the magnetic interfacial force, we may also define a magnetic Bond number, $Bo_{\mathrm{M}} := \mu_0 \chi H^2 d/\sigma$, although this does not take into account the variation of the normal component of $\mathbf{H}$ as a function of position along the interface. In our simulations we vary Bo_{M} at fixed Bo by varying $\mathbf{H}$ or χ, as given below.

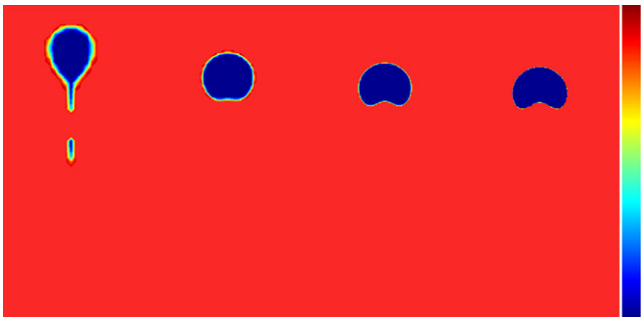

Figure 1. Rising bubble in a ferrofluid at numerical resolutions (left to right): 32×64, 64×128, 128×256, 256×512; here $\rho_1 = 2$, $\rho_2 = 1$, $\mu_1 = 0.02$, $\mu_2 = 0.01$, $\sigma = 0.003$ and $H = 1$.

Numerical convergence. We have found that adequate numerical accuracy is reached at moderate numerical resolution of approximately 128^2 computational nodes. In figure 1 we show a rising bubble at $t = 1$; the numerical resolution increases from left to right. Apart from the distinct sharpening of the interfacial region at higher resolution, it is apparent that the results in the final two cases are nearly identical. In the rightmost frame of figure 1 there are just over 100 cells across the bubble width (the entire computational domain is 256×512).

Rising bubbles. For these tests we adopt the following parameter values: $\sigma = 0.04$ N m^{-1}, $\rho_1 = 1000$ kg m^{-3}, $\rho_2 = 10$ kg m^{-3}, $\mu_1 = 0.01$ Pa s, $\mu_2 = 0.001$ Pa s and $R_{\mathrm{b}} = 1.5$ mm for the initial radius of the bubble. The field is uniform and oriented vertically (parallel to gravity). In this work we have attempted to choose realistic physical parameters for a ferrofluid and accompanying non-magnetic fluid (liquid or gas). However, numerical constraints have also guided some parameter choices, such as densities, because large ratios in density dramatically increase computation times.

As a result of the normal force acting on the interface in equation (4), the bubble will elongate along the direction of the field. This elongation is counteracted by: (i) interfacial tension, which tends to a state of uniform curvature; (ii) buoyancy forces; (iii) pressure variations and viscous stresses that vary along the bubble interface due to the rising motion. We see a preliminary result in figure 2, showing that the elongation leads to a drag reduction which in turn leads to faster rising bubbles (the times shown in the top and bottom frames in figure 2 are identical). This effect can be examined in more detail by increasing the field and taking snapshots of the rising at a fixed time $t_1 > 0$, as shown in figure 3. Other workers have seen similar behavior [21, 22].

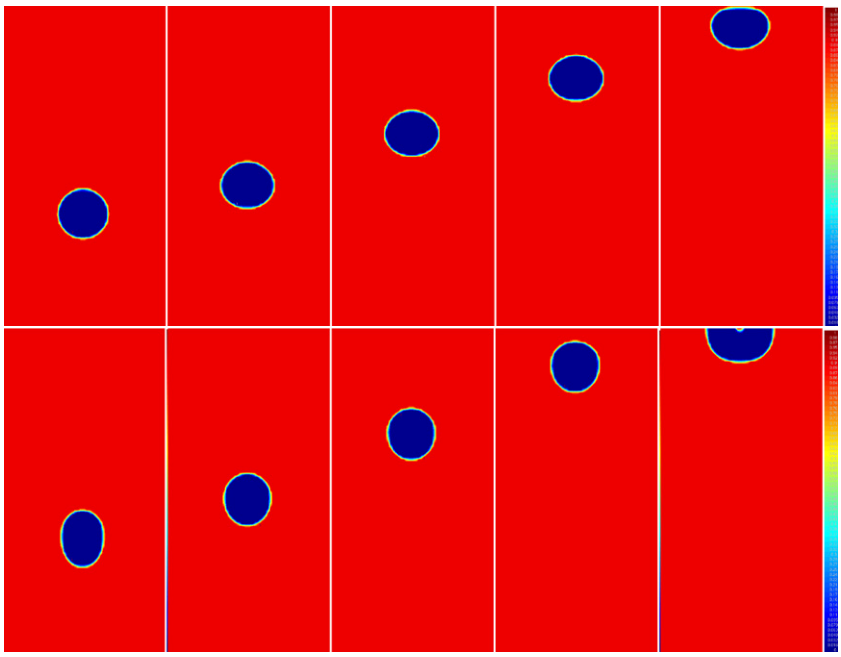

Figure 2. A bubble rising in ferrofluid, with (bottom row) and without (top row) a uniform vertical magnetic field.

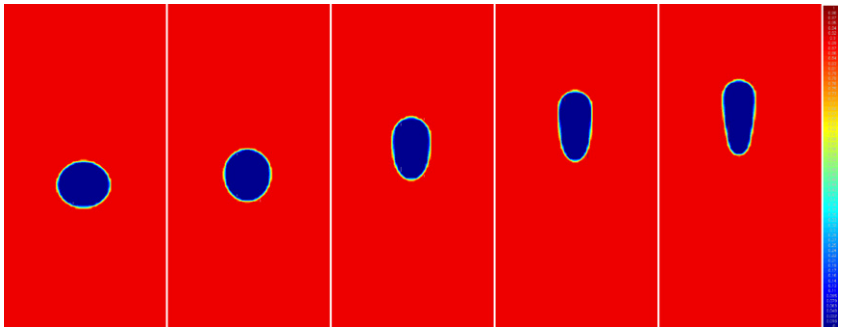

Figure 3. Effect of increasing field: $Bo_{\mathrm{M}} = 0, 1, 2, 3, 4$ (left to right) all shown at $t = 1$.

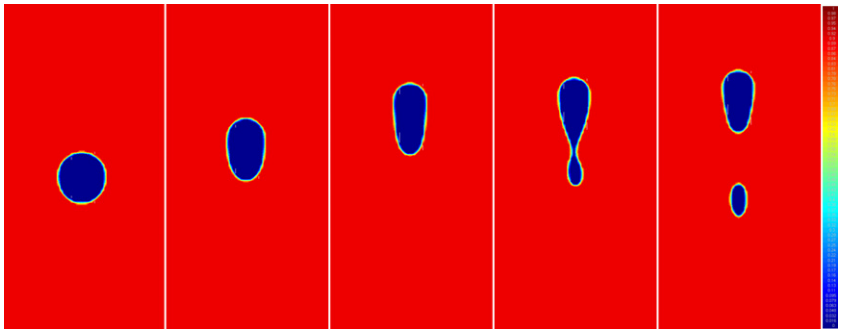

Figure 4. Effect of increasing susceptibility: $\chi = 1, 2, 3, 4, 5$ (left to right).

Alternatively, we can increase the susceptibility χ, seeing nearly identical effects, shown in figure 4, but for a larger range of magnetic forcing, exceeding the threshold where the bubble is driven to breakup.

Falling droplets. Because of their similar behavior, we present in this section a basic comparison between bubble and droplet behavior for the same conditions. For these tests we adopt the following parameter values: $\sigma = 0.01$ N m^{-1}, $\rho_1 = 2$ kg m^{-3}, $\rho_2 = 1$ kg m^{-3}, $\mu_1 = 0.05$ Pa s, $\mu_2 = 0.01$ Pa s, $\chi = 3$, and $R_{\mathrm{b}} = 1.5$ mm for the initial radius of the droplet and bubble. In figure 5 two asymmetries are apparent, between the bubble and droplet: first, the droplet has fallen more than the bubble has risen; and second, the bubble has become more

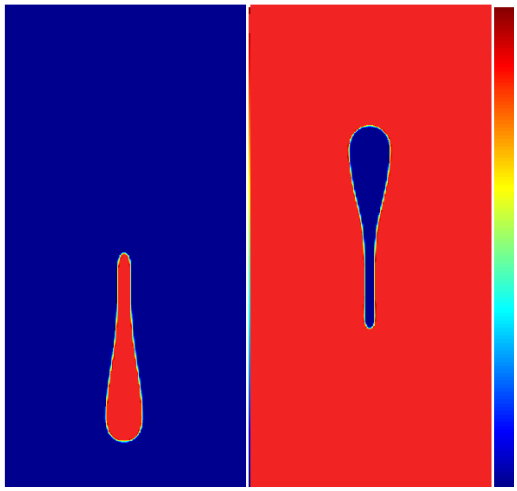

Figure 5. Falling droplet (left) versus rising bubble (right) in a uniform vertical field, under identical physical conditions.

elongated, as is most apparent in its more extended and thinner tail. The asymmetry is rise/fall time is due to ordinary added mass effects but the greater elongation of bubbles is due to the different magnetic interfacial stress, as discussed earlier. A slightly conical end is observable on the droplet; such shapes have been observed experimentally [2, 3].

5. Discussion and conclusions

We have developed and tested a VOF type code to simulate the dynamics of two-fluid flows of magnetic fluids with dynamic interfaces for uniform imposed magnetic fields. The code was applied to examine the shape change and rising and falling dynamics of bubbles and droplets of magnetic fluid in non-magnetic fluid for a range of physical parameters, always at small Bond number.

Collaborations are under way to image rising gas bubbles in ferrofluid using a high speed high resolution x-ray camera at the Advanced Photon Source, Argonne National Laboratory USA; initial tests have verified feasibility [23].

Other simulations (not shown here) of droplets and bubbles in zero gravity show that for higher field strengths, the droplet stretches out to form a 'popsicle stick' shape. Considering the close analogy between ferrofluid droplets and dielectric droplets [13], it is interesting that no experimental evidence for any tip-streaming like behavior in ferrodroplets has yet been recorded. Numerical simulations offer another avenue for exploring this possibility.

At present, we are conducting more extensive validation studies of the code based on the normal field instability [5] and are extending the model to axisymmetric and full three-dimensional versions.

Acknowledgment

We would like to thank Ron Rosensweig for enlightening discussions and comments.

References

[1] Arkhipenko V I, Barkov Yu D and Bashtovoi V G 1978 *Magnetohydrodynamics* **14** 373
[2] Bacri J-C and Salin D 1982 *J. Phys. Lett.* **43** L649
[3] Bacri J-C and Salin D 1983 *J. Phys. Lett.* **44** L415
[4] Clift R, Grace J R and Weber M E 1978 *Bubbles, Drops and Particles* (New York: Dover)
[5] Cowley M D and Rosensweig R E 1967 *J. Fluid Mech.* **30** 671
[6] Garton C G and Krasucki Z 1964 *Proc. R. Soc.* A **280** 211
[7] Lafaurie B, Nardonne C, Scardovelli R, Zaleski S and Zanetti G 1994 *J. Comput. Phys.* **113** 134
[8] Kao K C 1961 *Br. J. Appl. Phys.* **12** 629
[9] Landau L D and Lifshitz E M 1960 *Electrodynamics of Continuous Media* (Oxford: Pergamon)
[10] Mai J, Früh W G and Yamane R 2002 *J. Magn. Magn. Mater.* **252** 169
[11] Matthies G and Tobiska L 2005 *J. Magn. Magn. Mater.* **289** 346
[12] Melcher J R 1981 *Continuum Electromechanics* (Cambridge, MA: MIT Press)
[13] Melcher J R and Taylor G I 1969 *Annu. Rev. Fluid Mech.* **1** 111
[14] Miksis M J 1981 *Phys. Fluids* **24** 1967
[15] Rosensweig R E 1985 *Ferrohydrodynamics* (New York: Dover)
[16] Rudman M 1997 *Int. J. Numer. Methods Fluids* **24** 671
[17] Scardovelli R and Zaleski S 1999 *Annu. Rev. Fluid Mech.* **31** 567–603
[18] Sherwood J D 1988 *J. Fluid Mech.* **188** 133
[19] Stone H A, Lister J R and Brenner M P 1999 *Proc. R. Soc.* A **455** 329
[20] Taylor G I 1966 *Proc. R. Soc.* A **291** 159
[21] Ueno K, Higashitani M and Kamiyama S 1995 *J. Magn. Magn. Mater.* **149** 104
[22] Ueno K, Nishita T and Kamiyama S 1999 *J. Magn. Magn. Mater.* **201** 281
[23] Lee W-K 2007 private communication, Argonne